

# Quantum quenches in disordered systems: Approach to thermal equilibrium without a typical relaxation time

Ehsan Khatami,<sup>1</sup> Marcos Rigol,<sup>1</sup> Armando Relaño,<sup>2,3</sup> and Antonio M. García-García<sup>4,5</sup>

<sup>1</sup>*Department of Physics, Georgetown University, Washington, DC 20057, USA*

<sup>2</sup>*Departamento de Física Aplicada I, Universidad Complutense de Madrid, Av. Complutense s/n, 28040 Madrid, Spain*

<sup>3</sup>*Instituto de Estructura de la Materia, IEM-CSIC, Serrano 123, 28006 Madrid, Spain*

<sup>4</sup>*CFIF, Instituto Superior Técnico, Universidade Técnica de Lisboa, Av. Rovisco Pais, 1049-001 Lisboa, Portugal*

<sup>5</sup>*TCM Group, Cavendish Laboratory, University of Cambridge, JJ Thomson Avenue, Cambridge, CB3 0HE, UK*

We study spectral properties and the dynamics after a quench of one-dimensional spinless fermions with short-range interactions and long-range random hopping. We show that a sufficiently fast decay of the hopping term promotes localization effects at finite temperature, which prevents thermalization even if the classical motion is chaotic. For slower decays, we find that thermalization does occur. However, within this model, the latter regime falls in an unexpected universality class, namely, observables exhibit a power-law (as opposed to an exponential) approach to their thermal expectation values.

PACS numbers: 05.70.Ln, 72.15.Rn, 05.60.Gg, 71.30.+h

The study of the dynamics and conditions for thermalization in isolated many-body systems has a long history in theoretical physics [1]. In classical physics, the requirements for thermalization are well understood. Boltzmann's ergodic hypothesis holds only if the motion of the individual particles is fully chaotic. The situation in quantum systems is less clear. Quantum time evolution is described by a linear differential equation so that dynamical chaos does not occur. The development of the theory of quantum chaos in the 1980's and 1990's brought a new language and techniques to tackle this problem [2]. With respect to thermalization, this effort crystallized in two main results: the so-called Berry's hypothesis [3], which states that eigenstates of a classically chaotic system can be written as a finite sum of plane waves with random coefficients, and the eigenstate thermalization hypothesis (ETH) proposed by Deutsch [4] and Srednicki [5], which states that observables in individual eigenstates of a generic many-body system already exhibit thermal behavior.

Until a few years ago, technical difficulties prevented a systematic study of the proposals above. However, recent advances in cold gases systems, together with the enhancement of computer power and the development of novel computational methods, are making possible a more quantitative comparison. This has dramatically boosted the theoretical and experimental interest in non-equilibrium dynamics in general and thermalization in particular [6]. For instance, in Ref. [7], it was shown experimentally that, after a quench, the momentum distribution of a gas of bosons trapped in a quasi-one-dimensional (1D) geometry did not relax to the thermal prediction. Although this is expected in an integrable system [8], it was surprising that such an effect could be seen experimentally. The ETH, on the other hand, has been confirmed numerically for nonintegrable systems [9], and has been shown to break down when approaching integrable points [10–12].

A better understanding of the conditions for thermalization would not only put the foundation of quantum statistical mechanics on a more solid ground but also have a strong impact in different fields, from cold gases to cosmology, where non-equilibrium dynamics play a key role. Here, we provide

further insights on this problem. We show that many-body localization effects [13] invalidate the expectation that classical chaos leads to thermalization of the quantum counterpart. (For recent connections between the effect of localization in Fock space and thermalization in spin systems, see Ref. [14].) We also put forward a route toward thermalization in quantum systems characterized by power-law relaxation dynamics. We support these results by numerical calculations in the following 1D spinless fermions system, with long-range hopping and short-range interactions,

$$\hat{H} = \sum_{ij} J_{ij} \left( \hat{f}_i^\dagger \hat{f}_j + \text{H.c.} \right) + V \sum_i \left( \hat{n}_i - \frac{1}{2} \right) \left( \hat{n}_{i+1} - \frac{1}{2} \right), \quad (1)$$

where  $\hat{f}_j^\dagger$  creates a fermion in the site  $j$ , and  $\hat{n}_j$  is the number operator in the site  $j$ . The hopping term is built by means of a Gaussian random distribution, with zero mean  $\langle J_{ij} \rangle = 0$ , and

$$\langle (J_{ij})^2 \rangle = \left[ 1 + \left( \frac{|i-j|}{\beta} \right)^{2\alpha} \right]^{-1}. \quad (2)$$

In the limit  $V = 0$ , the properties of (1) depend on  $\alpha$  but not on  $\beta > 0$  [15]. For  $\alpha < 1$ , eigenstates are delocalized and the spectral correlations are described by Wigner-Dyson (WD) statistics. For  $\alpha > 1$ , eigenstates are localized and spectral correlations are described by Poisson statistics. For  $\alpha = 1$ , eigenstates are multifractal and spectral correlations are intermediate between WD and Poisson [16, 17]. We then fix  $\beta = 0.1$  and  $V = 1$ . (The latter sets the unit of energy throughout this Rapid Communication, and  $k_B = 1$ .) These values were chosen to minimize finite-size effects ( $\beta \ll 1$ ) and at the same time to avoid the trivial insulator limit that occurs if the potential energy is much larger than the kinetic one [11]. Likewise, if the interaction is too weak, thermalization may not occur [10]. Finally, we note that these types of long-range Hamiltonians have been used to model systems with strong dipolar interactions [18].

We first use a finite-size scaling analysis to investigate the effect of the many-body interactions on the spectrum [17].

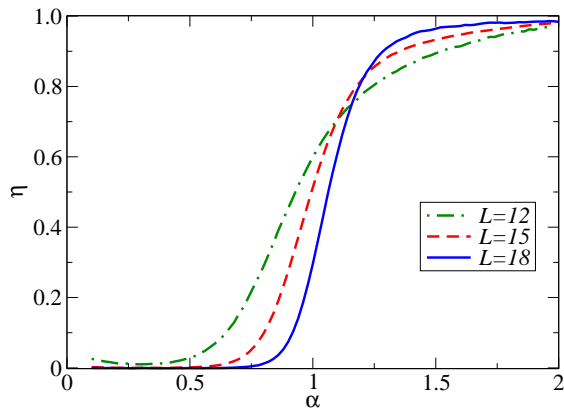


FIG. 1. (Color online) Scaling variable  $\eta$  [see Eq. (3)] as a function of  $\alpha$  for different system sizes but the same filling factor,  $1/3$ . For  $\alpha \lesssim 1$  ( $\alpha \gtrsim 1.2$ ),  $\eta$  decreases (increases) with the system size. This is a signature of a metallic (insulating) phase. The number of realizations is 10000, 10000, and 400 for  $L = 12, 15$ , and  $18$ , respectively.

This is a powerful tool to study many-body localization in the presence of interactions [11, 13]. We compute the eigenvalues of the Hamiltonian (1) for different sizes and values of  $\alpha$  utilizing standard diagonalization techniques. In all cases, the filling factor  $p/L = 1/3$ , where  $L$  is the system size and  $p$  is the number of particles. The spectrum thus obtained is appropriately unfolded, i.e., it is rescaled so that the spectral density on a spectral window comprising several level spacings is unity. The number of disorder realizations considered is such that statistical fluctuations are negligible. As a scaling variable we choose the function  $\eta$  [17] related to the variance  $\text{var} = \langle s^2 \rangle - \langle s \rangle^2$  of the level spacing distribution  $P(s)$ .  $P(s)$  is the probability of finding two neighboring eigenvalues at a distance  $s = (\epsilon_{i+1} - \epsilon_i)/\Delta$ , where  $\Delta$  is the local mean level spacing, and

$$\eta = [\text{var} - \text{var}_{\text{WD}}]/[\text{var}_{\text{P}} - \text{var}_{\text{WD}}]. \quad (3)$$

$\text{var}_{\text{WD}} = 0.286$  ( $\text{var}_{\text{P}} = 1$ ) is the value of the variance for a disordered metal (insulator) in the thermodynamic limit and  $\langle s^n \rangle = \int s^n P(s)$  [19]. An increase (decrease) of  $\eta$  with  $L$  signals that the system will be an insulator (metal) in the thermodynamic limit.

Figure 1 depicts results for  $\eta$  vs  $\alpha$  for different sizes. It is apparent that for  $\alpha \gtrsim 1.2$  the parameter  $\eta$  increases with system size, as is expected of an insulator. Hence, localization takes place in the interacting system, in contrast to the classical counterpart, which is chaotic for any  $\alpha$ . For  $\alpha \lesssim 1$ , on the other hand,  $\eta$  behaves as expected of a metal. To be certain whether the system is metallic for  $\alpha \approx 1$ , much larger systems, currently not accessible numerically, need to be studied.

We now investigate the thermalization properties of the Hamiltonian (1). We aim to (i) identify a region of  $\alpha$ 's for which the system does not thermalize even though the classical counterpart does, (ii) see how that region relates to the localization regime found by the spectral analysis, (iii) investigate the microscopic origin of the lack of thermalization, and (iv) study the approach to equilibrium in the region of  $\alpha$ 's for which thermalization eventually occurs.

In order to proceed, we first note that time scales and finite-size effects relevant to the study of quantum thermalization may depend on the observable and particle statistics [10, 12]. However, for few-body observables, it is generically expected that thermalization occurs away from integrability. Here, we report results for two of those observables: the momentum distribution function  $[\hat{n}(k)]$  and the density-density structure factor  $[\hat{N}(k)]$ ,

$$\hat{n}(k) = \frac{1}{L} \sum_{l,m} e^{ik(l-m)} \hat{f}_l^\dagger \hat{f}_m, \quad \hat{N}(k) = \frac{1}{L} \sum_{l,m} e^{ik(l-m)} \hat{n}_l \hat{n}_m, \quad (4)$$

which are the Fourier transforms of the one-particle and density-density correlation matrices [20], respectively. Both observables can be measured in ultracold gases experiments.

In all the cases shown below, we start from an eigenstate of the Hamiltonian (1) in a certain realization of the disorder. Then, we change to another disorder realization for the same  $\alpha$ , and study the time evolution of the initial state with this final Hamiltonian,  $\hat{H}_{\text{fin}}$ . This procedure is usually known as a quench. The initial state  $[|\Psi(0)\rangle]$  is selected such that the time evolving system has an energy  $E = \langle \Psi(0) | \hat{H}_{\text{fin}} | \Psi(0) \rangle$ , which, for every disorder realization, is the same as the one of a thermal state with temperature  $T = 10.0$  ( $E = \text{Tr}\{e^{-\hat{H}_{\text{fin}}/T} \hat{H}_{\text{fin}}\} / \text{Tr}\{e^{-\hat{H}_{\text{fin}}/T}\}$ ). This yields energies that fall close to the center of the spectrum of the final Hamiltonian. In what follows,  $O_{ij}$  are the matrix elements of a given observable in the eigenstates of the final Hamiltonian,  $O_{ij} = \langle \psi_i | \hat{O} | \psi_j \rangle$ , and  $C_j$  is the overlap between the initial state and  $|\psi_j\rangle$ ,  $C_j = \langle \psi_j | \Psi(0) \rangle$ .

In order to determine whether thermalization occurs following the quench, one needs to find a meaningful quantity to compare with the microcanonical (thermal) average,  $O_{\text{micro}} = \frac{1}{\mathcal{N}_{\Delta E}} \sum_j O_{jj}$ , where  $\mathcal{N}_{\Delta E}$  is the number of states in the microcanonical window (centered around  $E$ , and with  $\Delta E$  selected such that the average is robust against small changes of  $\Delta E$ ). If relaxation takes place for the observables of interest, and the spectrum is nondegenerate, the infinite time average (also known as the diagonal ensemble prediction)  $O_{\text{diag}} = \sum_j |C_j|^2 O_{jj}$  is the right choice [9]. We first compute the normalized difference between these two ensembles,

$$\Delta O = \frac{\sum_k |O_{\text{diag}}(k) - O_{\text{micro}}(k)|}{\sum_k O_{\text{diag}}(k)}, \quad (5)$$

and then average it over different disorder realizations to obtain  $\langle \Delta O \rangle_{\text{dis}}$ . Note that here, and in what follows, by “ $O$ ” we mean “ $n$ ” or “ $N$ ” for the momentum distribution and structure factor, respectively.

In Fig. 2, we depict  $\langle \Delta n \rangle_{\text{dis}}$  and  $\langle \Delta N \rangle_{\text{dis}}$  for different values of  $\alpha$  vs system size. Thermalization occurs if  $\langle \Delta O \rangle_{\text{dis}}$  vanishes in the thermodynamic limit. A nonzero value of  $\langle \Delta O \rangle_{\text{dis}}$  in this limit indicates that the observable  $O$  relaxes to a nonthermal expectation value. For  $\alpha > 1$ , a weak size dependence is observed for the largest system sizes we can study, with  $\langle \Delta O \rangle_{\text{dis}}$  likely saturating to non-zero values for  $\alpha \gtrsim 1.2$ . Therefore, thermalization is not expected to occur in this regime. Interestingly, as the value of  $\alpha$  decreases below  $\alpha \sim 1$ , the normalized differences exhibit a fast decrease for

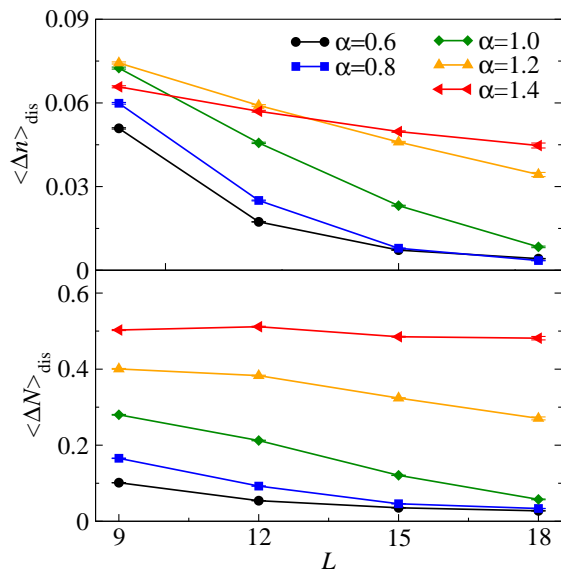


FIG. 2. (Color online)  $\langle \Delta n \rangle_{\text{dis}}$  and  $\langle \Delta N \rangle_{\text{dis}}$  [see Eq. (5)], as a function of the system size, for  $\alpha = 0.6, 0.8, 1.0, 1.2,$  and  $1.4$ . Points correspond to  $(L, p) = (9, 3), (12, 4), (15, 5),$  and  $(18, 6)$ . The disorder average is performed over at least 8,500 different realizations for  $L \leq 15$ , and 1020 for  $L = 18$ . The classical dynamics is chaotic but there is no thermalization for large  $\alpha$  due to localization effects.

the smallest systems shown. They become much smaller than those for  $\alpha \gtrsim 1.2$  for the largest system sizes accessible here, for which  $\langle \Delta O \rangle_{\text{dis}}$  is very close to zero within our error bars and still decreasing with increasing system size. These results suggest that thermalization occurs in this regime.

In order to further support the conclusions of the finite-size scaling analysis we look at the actual diagonal and microcanonical expectation values of observables for several quenches. Results for  $n(k=0)$  are shown in Fig. 3 as a function of the energy. In all regimes, the microcanonical results can be seen to be almost independent of the energy, while the diagonal ensemble results exhibit fluctuations that increase as  $\alpha$  increases. Hence, increasing  $\alpha$  increases the difference between the infinite time average and the microcanonical results, as well as increases the dependence of the infinite time average on the initial state selected.

A natural question that follows is whether the absence of thermalization, as well as the sensitivity to the initial state selected, for large  $\alpha$ , is related to the breakdown of ETH (as seen

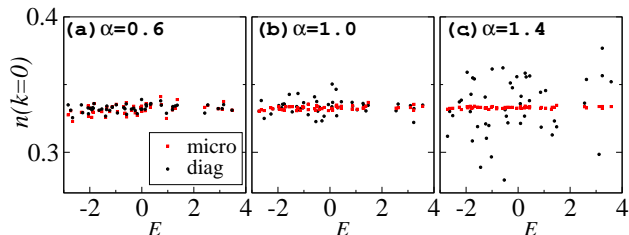


FIG. 3. (Color online) Microcanonical and diagonal results for  $n(k=0)$  in 51 different quenches. The systems have 18 sites and six particles, with  $\alpha = 0.6, 1.0,$  and  $1.4$ .

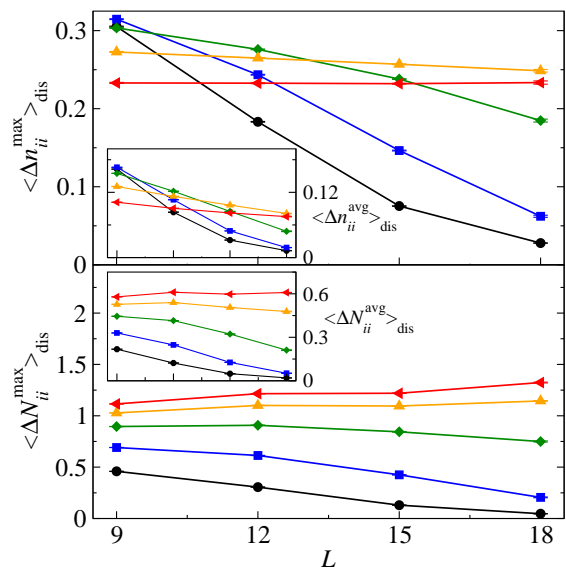


FIG. 4. (Color online)  $\langle \Delta n_{ii}^{\text{max}} \rangle_{\text{dis}}$  and  $\langle \Delta N_{ii}^{\text{max}} \rangle_{\text{dis}}$  (main panels), and  $\langle \Delta n_{ii}^{\text{avg}} \rangle_{\text{dis}}$  and  $\langle \Delta N_{ii}^{\text{avg}} \rangle_{\text{dis}}$  (insets) vs system size. Lines are the same as in Fig. 2. As a consequence of localization effects, ETH does not hold for large values of  $\alpha$ .

in clean systems approaching an integrable point [10, 11]) or it is rather related to some atypical properties of the overlaps  $C_j$ . To answer that question, we compute the normalized difference between the observable in each eigenstate and in the microcanonical ensemble,

$$\Delta O_{ii} = \frac{\sum_k |O_{ii}(k) - O_{\text{micro}}(k)|}{\sum_k O_{\text{micro}}(k)}. \quad (6)$$

This allows us to determine, for each disorder realization, the maximal difference within the microcanonical window  $\Delta O_{ii}^{\text{max}} = \text{Max}[\Delta O_{ii}]_{\Delta E}$  as well as the average  $\Delta O_{ii}^{\text{avg}} = \frac{1}{\mathcal{N}_{\Delta E}} \sum_i \Delta O_{ii}$ . We then average both quantities over different disorder realizations to obtain  $\langle \Delta O_{ii}^{\text{max}} \rangle_{\text{dis}}$  and  $\langle \Delta O_{ii}^{\text{avg}} \rangle_{\text{dis}}$ .

In the main panels in Fig. 4, we depict  $\langle \Delta n_{ii}^{\text{max}} \rangle_{\text{dis}}$  and  $\langle \Delta N_{ii}^{\text{max}} \rangle_{\text{dis}}$  vs  $L$  for different values of  $\alpha$ . ETH holds when  $\langle \Delta O_{ii}^{\text{max}} \rangle_{\text{dis}} \rightarrow 0$  for  $L \rightarrow \infty$ . In the range of sizes that we can study, this behavior is apparent for  $\alpha \lesssim 1$ . For  $\alpha \gtrsim 1.2$ , we find clear indications that ETH fails, which can be understood as a result of localization induced by disorder [13]. A very similar behavior is observed in the insets of Fig. 4, which show  $\langle \Delta n_{ii}^{\text{avg}} \rangle_{\text{dis}}$  and  $\langle \Delta N_{ii}^{\text{avg}} \rangle_{\text{dis}}$ . In the region  $\alpha \approx 1$ , on the other hand, our results are not conclusive. This is an interesting problem for future works as, in the noninteracting limit,  $\alpha = 1$  corresponds to a metal-insulator transition characterized by multifractal eigenstates. We speculate that fluctuations at all scales associated with multifractality may lead to interesting behavior in the many-body properties of the system.

The robustness of the results for  $\langle \Delta O_{ii}^{\text{max}} \rangle_{\text{dis}}$  and  $\langle \Delta O_{ii}^{\text{avg}} \rangle_{\text{dis}}$ , as well as their clear correlation with the thermalization indicators in Fig. 2, allow us to conclude that: (i) the lack (occurrence) of thermalization is directly related to the failure (validity) of ETH, and (ii) that ETH holds and thermalization occurs only for values of  $\alpha \lesssim 1$ . For  $\alpha$  greater than, and not

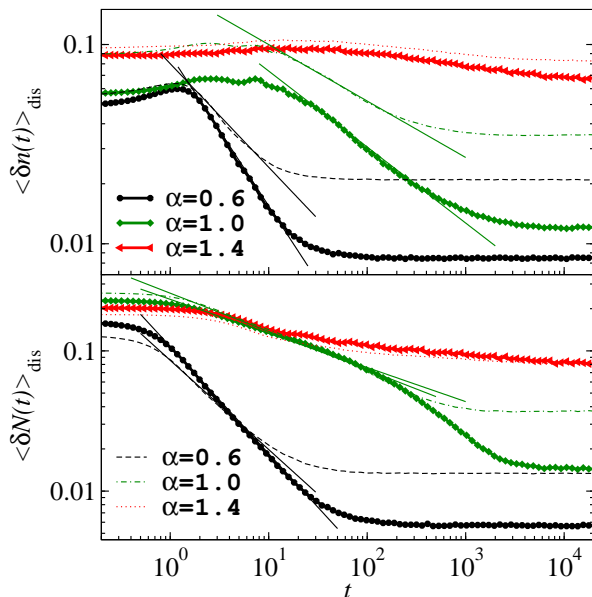


FIG. 5. (Color online) Time evolution of  $\langle \delta n(t) \rangle_{\text{dis}}$  and  $\langle \delta N(t) \rangle_{\text{dis}}$  [see Eq. (7)] for different  $\alpha$ 's. Thick lines are for 18 sites and six particles. Thin solid lines are power-law fits to the data. Other thin lines are the corresponding results for 15 sites and five particles. An average over 8500 (1020) realizations has been carried out for the 15-site (18-site) system.

too close to, one, the quantum system will not thermalize even though the dynamic of the classical counterpart is chaotic.

A fundamental problem that has not been addressed in previous computational studies—due to large fluctuations that occur during the time evolution in exact diagonalization studies (because of finite-size effects) and to the limited times accessible in time-dependent density-matrix renormalization group (t-DMRG) approaches [21]—is that of how observables approach their thermal values during the relaxation dynamics. The naive expectation is that the approach should be exponential as in classical systems, where a few collisions per particle suffice for the system to relax to thermal equilibrium. However, to the best of our knowledge, such a behavior has yet to be seen in the experiments or numerical simulations of isolated systems in the quantum regime. Disordered systems provide a unique opportunity to address this problem as the average over disorder realizations reduces dramatically fluctuations due to finite-size effects. In what follows, we compute the time evolution of the difference

$$\delta O(t) = \frac{\sum_k |O(k,t) - O_{\text{diag}}(k)|}{\sum_k O_{\text{diag}}(k)}, \quad (7)$$

and then average it over different disorder realizations to obtain  $\langle \delta O(t) \rangle_{\text{dis}}$  [10]. In Fig. 5, we show results for  $\langle \delta n(t) \rangle_{\text{dis}}$  and  $\langle \delta N(t) \rangle_{\text{dis}}$  as a function of time,  $t$ , for three different values of  $\alpha$  and the two largest system sizes that we can study. For  $\alpha > 1$ , an extremely slow relaxation dynamics can be observed, and the system may never reach the infinite time-average prediction in any experimentally relevant time scale. For  $\alpha \lesssim 1$ , the relaxation dynamics seen in those plots is quite unexpected. We find that  $\langle \delta n(t) \rangle_{\text{dis}}$  and  $\langle \delta N(t) \rangle_{\text{dis}}$  exhibit a clear power-law decay ( $\propto t^{-\gamma}$ ). The region over which the power-law decay is observed extends over a decade and increases with increasing system size. As the value of  $\alpha$  decreases (and localization effects decrease) the exponent  $\gamma$  of the power law increases. However, no typical time-scale emerges during relaxation [22]. This indicates an unexpected route to thermal equilibrium in many-body quantum systems characterized by a power law rather than an exponential decay.

After these results, it is natural to speculate whether such power-law behavior also occurs in clean systems. Theoretically, it is well known that in the semiclassical limit classical cantori [23], remnants of the Kolmogorov-Arnold-Moser (KAM) tori induce slow diffusion in phase space and power-law localization of eigenstates in the one-body problem [24]. Therefore, it is plausible that in certain region of parameters the approach to equilibrium in systems controlled by cantori is also power-law-like. Interestingly, indications of power-law relaxation have already been seen in classical systems [25] and, experimentally, in a strongly correlated one-dimensional Bose gas [26].

In conclusion, we have studied an interacting many-body disordered system that exhibits a transition between metallic and insulating behavior. Remarkably, we have identified a region of parameters ( $\alpha \gtrsim 1.2$ ) in which, due to localization effects, ETH fails and thermalization does not take place even if the system is nonintegrable [14]. For  $\alpha \lesssim 1$ , ETH is valid and thermalization occurs. Furthermore, in the latter regime, we have found a route toward thermal equilibrium characterized by a power-law approach to the thermal expectation values and, hence, by the lack of a well-defined equilibration time. The relevance of this scenario to experiments with ultracold gases, as well as clean strongly correlated systems, is a topic that requires future exploration.

This research was supported by NSF under Grant No. OCI-0904597 (E.K. and M.R.) and by the U.S. Office of Naval Research (M.R.). A.M.G. acknowledges support from Galileo Galilei Institute, FCT (PTDC/FIS/111348/2009), Marie Curie Action (PIRG07-GA-2010-26817), and EPSRC (EP/I004637/1). A.R. acknowledges support from the Spanish Government Grants No. FIS2009-11621-C02-01 and No. FIS2009-07277.

- [1] L. Boltzmann, *Creeles J.* **98**, 68 (1884).  
 [2] H. J. Stockmann, *Quantum Chaos: An Introduction*, (Cambridge University Press, Cambridge, U.K., 1999).  
 [3] M. V. Berry, *J. Phys. A: Math. Gen.* **10**, 2083 (1977).  
 [4] J. M. Deutsch, *Phys. Rev. A* **43**, 2046 (1991).

- [5] M. Srednicki, *Phys. Rev. E* **50**, 888 (1994).  
 [6] M. A. Cazalilla and M. Rigol, *New J. Phys.* **12**, 055006 (2010); A. Polkovnikov, K. Sengupta, A. Silva, and M. Vengalattore, *Rev. Mod. Phys.* **83**, 863 (2011).  
 [7] T. Kinoshita, T. Wenger, and D. S. Weiss, *Nature (London)* **440**,

- 900 (2006).
- [8] M. Rigol, V. Dunjko, V. Yurovsky, and M. Olshanii, Phys. Rev. Lett. **98**, 050405 (2007); M. Rigol, A. Muramatsu, and M. Olshanii, Phys. Rev. A **74**, 053616 (2006).
- [9] M. Rigol, V. Dunjko, and M. Olshanii, Nature (London) **452**, 854 (2008).
- [10] M. Rigol, Phys. Rev. Lett. **103**, 100403 (2009); Phys. Rev. A **80**, 053607 (2009).
- [11] L. F. Santos and M. Rigol, Phys. Rev. E **81**, 036206 (2010); Phys. Rev. E **82**, 031130 (2010).
- [12] C. Neuenhahn and F. Marquardt, arXiv:1007.5306; G. Roux, Phys. Rev. A **81**, 053604 (2010).
- [13] D. M. Basko, I. L. Aleiner, and B. L. Altshuler, Ann. Phys. **321**, 1126 (2006); V. Oganesyan and D. A. Huse, Phys. Rev. B **75**, 155111 (2007); A. Pal and D. A. Huse, Phys. Rev. B **82**, 174411 (2010); C. Monthus and T. Garel, Phys. Rev. B **81**, 134202 (2010).
- [14] C. Gogolin, M. P. Muller, and J. Eisert, Phys. Rev. Lett. **106**, 040401 (2011); E. Canovi, D. Rossini, R. Fazio, G. E. Santoro, A. Silva, Phys. Rev. B **83**, 094431 (2011).
- [15] A. D. Mirlin, Y. V. Fyodorov, F.-M. Dittes, J. Quezada, and T. H. Seligman, Phys. Rev. E **54**, 3221 (1996); E. Cuevas, M. Ortuño, V. Gasparian, and A. Pérez-Garrido, Phys. Rev. Lett. **88**, 016401 (2001); I. Varga, Phys. Rev. B **66**, 094201 (2002).
- [16] S. M. Nishigaki, Phys. Rev. E **59**, 2853 (1999).
- [17] B. I. Shklovskii, B. Shapiro, B. R. Sears, P. Lambrianides, and H. B. Shore, Phys. Rev. B **47**, 11487 (1993); A. M. Garcia-Garcia and E. Cuevas, *ibid.* **75**, 174203 (2007).
- [18] L. S. Levitov, Phys. Rev. Lett. **64**, 547 (1990).
- [19] E. Cuevas, Phys. Rev. Lett. **83**, 140 (1999), E. Cuevas, E. Louis, and J. A. Vergés, *ibid.* **77**, 1970 (1996).
- [20] Since we work at fixed number of fermions  $p$ ,  $\langle \hat{N}(k=0) \rangle = p^2/L$ , so we set it to zero without any loss of generality.
- [21] C. Kollath, A. M. Läuchli, and E. Altman, Phys. Rev. Lett. **98**, 180601 (2007); S. R. Manmana, S. Wessel, R. M. Noack, and A. Muramatsu, *ibid.* **98**, 210405 (2007).
- [22] In this regime, based on the comparison between results obtained for different system sizes, the saturation observed for sufficiently long times is expected to be a finite-size effect.
- [23] R. S. MacKay, J. D. Meiss, and I. C. Percival, Phys. Rev. Lett. **52**, 697 (1984); W. Li and P. Bak, *ibid.* **57**, 655 (1986).
- [24] A. M. Garcia-Garcia and J. Wang, Phys. Rev. Lett. **94**, 244102 (2005); D. Wintgen and H. Marxer, *ibid.* **60**, 971 (1988); B. Hu, B. Li, J. Liu, and Y. Gu, *ibid.* **82**, 4224 (1999).
- [25] See, for example, B. J. Alder and T. E. Wainwright, Phys. Rev. A **1**, 18 (1970).
- [26] S. Trotzky, Y.-A. Chen, A. Flesch, I. P. McCulloch, U. Schollwöck, J. Eisert, and I. Bloch, Nature Phys. **8**, 325 (2012).